Diffusion and Cluster Formation in One-Dimensional Systems with Attractive Interactions

L. E. Helseth*

School of Physical and Mathematical Sciences, Division of Physics and Applied Physics, Nanyang Technological University, Singapore

Received: February 1, 2006

We study cluster formation in a finite one-dimensional model system where the particles experience long-range attractive forces. The particles are first placed in equidistant positions by a repulsive potential, which then is turned off, and only a weak long-range potential acts between the particles. It is shown that the mean-square deviation in distance between the colloids at first increases due to normal Brownian motion, followed by a crossover to anomalous diffusion governed by the long-range forces. Moreover, we also found that the subsequent cluster formation could be described by a Poisson distribution. The results presented here may help us understand diffusion and cluster formation in one-dimensional systems.

1. Introduction

A variety of colloidal structures can now be routinely reproduced by using various self-assembly techniques.[1−12] The self-assembled structures exhibit a wide range of physical properties and show novel responses in external magnetic or electric fields. Capillary, electric, and magnetic forces have proven particularly useful for assembling structures ranging from nanometer to millimeter scale both on solid−liquid and air−water interfaces and therefore give an additional degree of freedom.[5−14]

A major task is to understand the factors that rule such self-assembly in one, two, and three dimensions. Considerable work has been done, in particular, when it comes to two- and three-dimensional systems.[15−21] However, we are not aware of similar studies on one-dimensional systems, and it appears that a fundamental understanding of one-dimensional cluster formation is still lacking. This is partially related to the lack of suitable model systems and also due to the fact that, until recently, one-dimensional systems did not receive as much attention as their higher dimensional counterparts. However, it has been realized that one-dimensional colloidal assemblies may have a number of applications in, e.g., microfluidics and molecular electronics, thus boosting the research in this field.[22,23]

Here we present a model system for investigating cluster formation in reduced dimensions and demonstrate a number of interesting phenomena. The particles are first placed in equidistant positions by a repulsive potential that can be turned on or off by remote operation. Also present is a weak long-range capillary force that acts between the particles and tends to create clusters in the absence of other repulsive forces. It is shown that the mean-square deviation in distance between the colloids at first increases due to normal Brownian motion, followed by a crossover to anomalous diffusion governed by the long-range forces. Moreover, we found that the cluster formation can be described as a Poisson process. The results presented here may help us understanding diffusion and cluster formation in one-dimensional systems.

2. Experimental Methods

Carboxyl-modified superparamagnetic polystyrene beads of radius $a = 1.4\ \mu$m (M270) were purchased from Dynal. The paramagnetic beads had an effective susceptibility of $\chi = 0.17$ and were supplied at a density of 2×10^9 beads/ml and have zero magnetic moment in the absence of external magnetic fields. The cover glass was cleaned excessively with pure, deionized water. The paramagnetic beads were cleaned and dispersed in pure, deionized water at a density 6×10^7 beads/ml before use. A small droplet of this colloidal suspension of diameter of about 5 mm was deposited on top of the cover glass. The colloids were observed with a Leica microscope in transmission mode, and the droplet was protected from external air flow as much as possible by appropriate screening of the microscope.

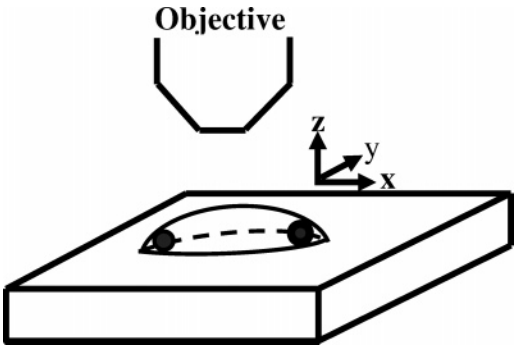

Figure 1. Schematic drawing of the system under study.

We noticed that the three-phase contact angle (air/water/glass) was typically 30°. It could be reduced to less than 10° by first treating the glass slides with 1 M NaOH ($T = 363$ K for 30 min), followed by a water wash, a bath in 1 M HCl (10 min), and finally, a thorough rinse in water.

A schematic drawing of the setup is displayed in Figure 1. The beads eventually approach the solid−water interface due to gravity, but do not stick due to electrostatic double-layer repulsion. The beads are therefore not in close contact with the glass slide, but instead levitate a small distance above it. After a while, some of the beads reach the three-phase contact line due to diffusion or slow evaporation-induced flow, where they are attracted to each other due to capillary forces. The beads are located at the air−water interface at a distance U from the three-phase contact line. As seen in Figure 2, a colloid approaching the three-phase contact line must deform the liquid surface slightly. When two colloids come together, the corre-

* Corresponding author. E-mail: lars@ntu.edu.sg.

10.1021/jp060678m CCC: $33.50
Published on Web 03/11/2006

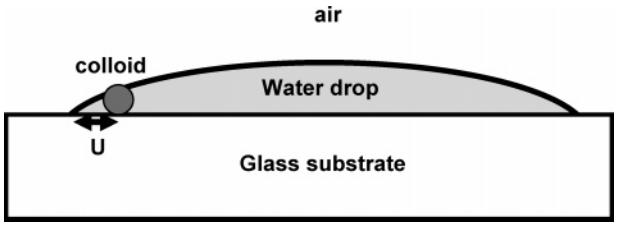

Figure 2. Schematic drawing showing how a single colloid deforms the liquid surface upon approaching the three-phase contact line.

sponding liquid surface deformations interact, causing an attractive capillary force between the colloids. As a result of their magnetic properties, the beads will repel each other when placed in a magnetic field perpendicular (in the *z* direction) to the glass substrate. In fact, the magnetic repulsive force can be tuned accurately by the external field, thus balancing the attractive capillary force and placing them in a periodic array, as seen in Figure 3a. If we turn off the magnetic field, the particles will again attract each other, thus resulting in clusters as in Figure 3b. We carefully selected experiments where evaporative flow did not alter the bead motion. The droplets used in the current study dried up after typically 2−4 h. All of the experiments reported here were done within 60 s, which means that the very slow evaporative flow does not influence the results. Moreover, all the experiments reported here were done within 60 s, and care was taken to avoid flow of more beads to the contact line after turning off the magnetic field.

3. Forces in the System

To understand the system at hand, we first determined the capillary forces by using the method of refs 3, 4. We deposited a droplet on a cover glass as described above and looked for two beads isolated from all the other beads. Initially, the beads are in close contact in a zero magnetic field. By increasing the external magnetic field *H*, the repulsive magnetic forces between these two beads also increase accordingly, and the dipolar force acting between two particles separated by a distance *D* is given by

$$F_{\mathrm{M}} = \frac{4\pi\chi^2 a^6 \mu_0 H^2}{3D^4} \tag{1}$$

where μ_0 is the permeability of water. On the other hand, the attractive capillary force between two colloids is given by[2,3]

$$F = A\left(\frac{1}{D} - \frac{D}{D^2 + 4U^2}\right) \tag{2}$$

where

$$A = 2\pi\delta^2\sigma / \left[\ln\left(\frac{2U}{a}\right)\right]^2$$

is a constant, *U* is the distance from the center of the colloids to the contact line, $\sigma = 72$ mN/m is the surface tension of water, and δ is the deformation of the water surface due to the colloids. By measuring the distance *D* for a given magnetic field *H*, we can determine the magnetic force F_{M} by using eq 1. In equilibrium, we have $F_{\mathrm{M}} = F$, which gives us an opportunity to measure *F* by tuning F_{M} by using an external magnetic field. Note that, because the colloids are performing Brownian motion, we need to take the average. The measurement procedure was described in detail in refs 2, 3. Figure 4 shows the force *F* as function of *D* when $U = 4.5$ μm (circles) and $U = 45$ μm

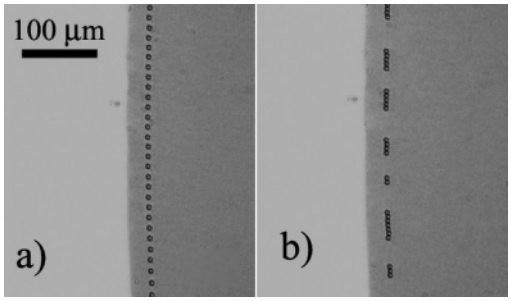

Figure 3. In (a), the colloids are distributed in a periodic array due to the repulsive magnetic force (magnetic field is on). In (b), the colloids have started forming clusters about 15 s after turning off the magnetic force.

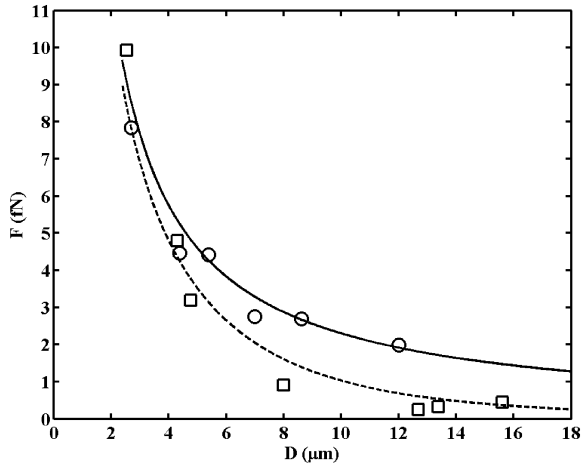

Figure 4. The capillary force as a function of distance when $U = 4.5$ μm (squares) and $U = 45$ μm (circles). The solid and dashed lines show the corresponding to theoretical fits using eq 2.

(squares). The solid and dashed lines show the corresponding fits using eq 2, with $A = 2.3 \times 10^{-20}$ J. This gives a deformation of the order of $\delta \sim 1$ nm, using the relationship between *A* and δ. Care should be taken when interpreting δ as above because we rely on a relationship between *A* and δ that is strictly valid only for point particles. However, it is reasonable to conclude that the surface deformation is on the nanometer scale. If it was much larger, the capillary forces would also scale accordingly, in contradiction with the very small forces we observe. The force in Figure 4 is slightly lower than that of ref 2, which could be explained by the fact that the colloids used here come from a different batch of those of ref 2 (they are all from the same supplier, Dynal). Here it is important to note that *A* depends strongly on the wetting properties of the individual colloids, which can be easily altered by small changes in surfactant density or surface charge on the colloids. These parameters may vary slightly from batch to batch and from colloid to colloid because colloids never are completely identical. Note that, for a smaller *U*, the capillary force falls off more quickly and the second term in eq 2 plays an important role. The distance *U* between colloids and the contact line is mostly controlled by the three-phase contact angle. In the rest of this study, we selected drops where $U > 10$ μm, in which case, the second term in eq 2 plays no essential role, and the capillary force is a long-range force proportional to $1/D$. Both dispersion and electrostatic forces play an important role at short distances between colloidal particles. The dispersion forces are important only for nanometer-range interparticle distances. On the other hand, the electrostatic forces play a role also at longer distances. The electrostatic interaction energy between two colloidal

surfaces can to a good approximation be described by $B\exp(-\kappa z)$, where B is a constant that depends on the electrostatic potentials of the two surfaces and κ is the Debye parameter.[24] If we insert the beads in pure water with $[H^+] = [OH^-] = 10^{-7}$ M and permittivity $\epsilon = 78$, we may expect B to be in the range of kT because the beads in 2D suspensions are often seen to collide but not attach to each other. Here k is Boltzmann's constant, T is the temperature in Kelvin and $1/\kappa \sim 500$ nm for pure water, which means that the electrostatic force falls off from $8fN$ at $z = 0$ μm to $1fN$ at $z = 1$ μm. Because the capillary forces are larger than this, we expect that only long-rang capillary forces are of importance here. However, these are just theoretical speculations. The real evidence that the dispersion and electrostatic forces do not play influential roles comes from Figure 4. Here it is seen that the total attractive force between the colloids is very well modeled by a $1/R$ force (i.e., the capillary force). Any additional short-range force (which decays faster than the capillary force) should easily be detected in Figure 4 when R decreases. However, no such change in the dependence of R is seen, and we are led to conclude that only the capillary forces play an important role.

4. Short-Time Diffusion

We first studied the short-time diffusion behavior of the system because it is crucial for our understanding of cluster formation. The colloids were initially placed in a periodic array as in Figure 3a. We then turned off the magnetic field so that only the long-range capillary forces were of importance. In each experiment, about 35 beads were in the field of view, and a total of six experiments were conducted. We prepared the colloids so that they were initially located a distance $R_i \approx 6$ μm apart (note that the distance between the colloids in an array is characterized by R_i to distinguish them from the distance D between two isolated colloids). We then measured the distance R_i between individual colloids with time intervals of $^1/_3$ s after removal of the magnetic field. Figure 5 shows the average distance R_m between the colloids as function of time t after the magnetic field has been turned off. The average distance between the colloids is defined as the sum over all separation distances between neighbor colloids divided by the number of colloids. This quantity does not change as a function of time because the system size (i.e., the distance between the first and the last colloid) does not change significantly. We notice that $R_m \approx 6$ μm is nearly constant over the whole time interval, as expected.

The mean-square deviation of the particle separations is found from the relationship

$$\sigma_R{}^2 = \frac{1}{N}\sum_{i=1}^{N}(R_i - R_m)^2 \qquad (3)$$

where N is the total number of measurements for each time frame ($N = 208$). The squares of Figure 6 display mean-square deviation as a function of time. It is important to emphasize that $\sigma_R(t = 0) \neq 0$ because the magnetic forces are unable to align the colloids perfectly. Initially ($t < 1$ s), it appears that the mean-square deviation increases linearly according to the equation

$$\sigma_R{}^2 \approx B + D_a t \qquad (4)$$

where the dashed line of Figure 6 shows eq 4 with $B = 0.25$ μm^2 and $D_a = 0.50$ μm^2/s. We notice that eq 4 is the normal diffusion equation with an offset term B. When $t > 1$ s, we

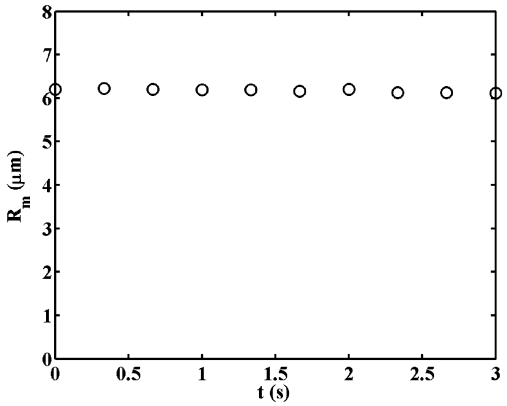

Figure 5. The average distance between the colloids as a function of time after turning off the magnetic field.

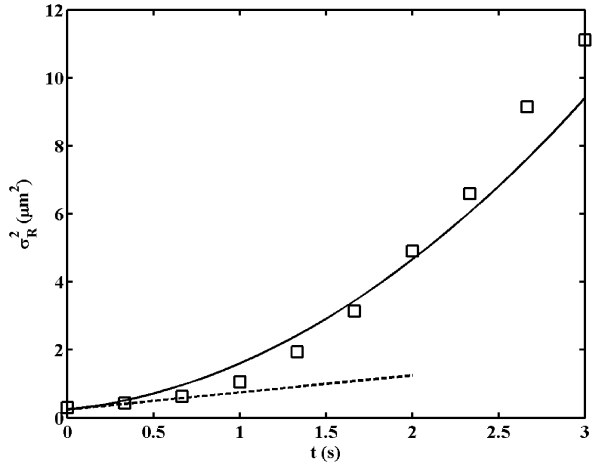

Figure 6. The mean-square deviation in distance between the colloids first increases linearly with time due to normal diffusion. After about 1 s, there is a crossover to anomalous diffusion. See text for details.

observe a crossover to anomalous diffusion, which to second order (in t) can described by

$$\sigma_R{}^2 \approx B + D_a t + D_b t^2 \qquad (5)$$

where the solid line of Figure 6 shows eq 5 with $D_b = 0.40$ μm^2/s^2. It is clear that capillary forces play a role here because $D_a \sim D_b$.

A theoretical model for the diffusion can be found by assuming that only nearest neighbors interact. We consider a large array of N particles, where the distance between particle k and $k-1$ is $L_k = d + x_k - x_{k-1}$, whereas the distance between particle k and $k+1$ is $L_{k+1} = d + x_{k+1} - x_k$. Here x_k is the local deviation of particle k from its equilibrium position and is caused entirely by the stochastic motion of the particle. The force on particle k from particles $k-1$ and $k+1$ can be given as

$$F_k(x_k) = F_k(L_{k+1}) - F_k(L_k) \approx (x_{k+1} - 2x_k - x_{k-1})\left(\frac{dF}{dL}\right)_{L=d} \qquad (6)$$

where we expanded to first order, assuming that the distance between the particles only performs small excursions about the equilibrium distance d. Note that the capillary force is attractive, so that $(dF/dL)_{L=d} < 0$. In presence of thermal fluctuations, the classical Langevin equation can be written as

$$\eta f a\frac{dx_k}{dt} = (x_{k+1} - 2x_k - x_{k-1})\left(\frac{dF}{dL}\right)_{L=d} + g_k(t) \qquad (7)$$

where η is the viscosity of water, f is the drag coefficient, and $g_k(t)$ is the stochastic force acting on particle k with an average zero and a correlation given as

$$\langle g_k(t_1) g_k(t_2) \rangle = \frac{kT}{\eta f a} \delta(t_1 - t_2) \tag{8}$$

where k is Boltzmann's constant, $T = 300$ K is the temperature, $\eta = 0.8 \times 10^{-3}$ Ns/m^2 is the viscosity of water, and f is the hydrodynamic drag coefficient ($f = 6\pi$ for a sphere in bulk liquid). Note that $\langle\ \rangle$ denotes the average and $\delta(t)$ is the delta function. The discrete Fourier transform (DFT) of x_k is defined as

$$\tilde{X}_n = \sum_{k=0}^{N-1} x_k \exp(j2\pi nk/N) \tag{9}$$

and can be used to transform eq 7 into[25]

$$\frac{d\tilde{X}_n(t)}{dt} = -\omega_n \tilde{X}_n(t) + \frac{1}{\eta f a} G_n(t) \tag{10}$$

where $G_n(t)$ is the DFT of the stochastic force and the characteristic frequency of the nth mode is given by

$$\omega_n = \frac{2}{\eta f a} \left(\frac{dF}{dL}\right)_{L=d} \left[1 - \cos\left(\frac{2\pi n}{N}\right)\right] \tag{11}$$

Note that we have assumed an infinite system, which is a reasonable assumption due to the many colloids involved. If we further assume that all the colloids are perfectly aligned at $t = 0$, $X_n(t = 0) = 0$, we obtain the following solution of eq 10:

$$\tilde{X}_n(t) = \frac{\exp(-\omega_n t)}{\eta f a} \int_0^t G_n(t_1) \exp(\omega_n t_1)\, dt_1 \tag{12}$$

Here we are mainly interested in the mean-square deviation (MSD), which is defined as

$$\sigma_R{}^2 = \frac{1}{N} \sum_{k=0}^{N-1} [L_k(t) - d]^2 \tag{13}$$

which can be evaluated by using Parceval's theorem

$$\sigma_R{}^2 = 2 \sum_{n=1}^{N-1} \langle \tilde{X}_n{}^2 \rangle \tag{14}$$

The reason for the factor of 2 in eq 14 is that we have measured the distance between the colloids, not their absolute positions. We emphasize that, at $t = 0$, the array of beads is not perfectly aligned, which can be described by a roughness (mean-square deviation) B. By using eq 9, we can transform eq 13 into

$$\sigma_R{}^2 = B + 2 \sum_{n=1}^{N-1} \langle \tilde{X}_n{}^2 \rangle \tag{15}$$

To obtain eq 14, we assumed that each particle is subjected to stochastic motion independently of each other. We point out that their motion is still correlated due to the long-range capillary forces, but that the water molecules colliding with the colloids (thus causing the stochastic variations) hit at random times and therefore do not "know" about the colloidal interaction force. Moreover, we note that the 0th Fourier mode does not contribute to the diffusion and has therefore been neglected. By using eqs 12 and 15, we find

$$\sigma_R{}^2 = B + \frac{2kT}{N\eta f a} \sum_{n=1}^{N-1} \frac{1 - \exp(-2\omega_n t)}{\omega_n} \tag{16}$$

Note that our expression is only valid as long as t is small ($t \ll 1/\omega_n \approx 5$ s) because, for larger t, the particles perform large excursions about the equilibrium distance d. This observation allows us to expand eq 13 to second order such that

$$\sigma_R{}^2 \approx B + 4D_1 t + 8D_2 t^2 \tag{17}$$

where $D_1 = kT/\eta f a$ and

$$D_2 \approx \left| \frac{D_1}{\eta f a} \left(\frac{dF}{dL}\right)_{L=d} \right| \tag{18}$$

We emphasize that D_1 is just the diffusion coefficient predicted by Einstein, whereas D_2 is a new diffusion coefficient needed to account for the interaction between the colloids. In eqs 17 and 18, we have made use of the fact that $(dF/dL)_{L=d} < 0$, so that the third term in eq 17 is always positive.

We can understand eq 17 by noting that each bead is at first located in a periodical array where the capillary forces nearly cancel each other. Thus, only thermal excitations on individual beads play a role, and these can be described by the normal diffusion equation. However, the array is soon brought out of its unstable equilibrium state by small perturbations, and the capillary forces come into play.

If we assume that $f = 6\pi$, it is easy to show that $D_1 \approx 0.2$ μm^2/s, i.e., a factor of 1.6 larger than $D_a/4$. This result suggests that beads experience a lower hydrodynamic drag than expected, which could be the case if they are only partially submerged in water (i.e., parts of them are in the air). By using eq 18, we estimate that $D_2 \approx 0.02$ μm^2/s^2. We then see that $8D_2 \approx 0.16$ μm^2/s^2, which is a factor 2.5 smaller than the measured value D_b. This discrepancy between theoretical and experimental values could be related to the fact that we have neglected interactions between next nearest neighbors.

5. Cluster Formation

The first clusters are observed to occur after about $t = 5$ s, which means that the motion of each individual bead in the cluster is correlated. To this end, an interesting question is how the distribution of clusters changes with time. To answer this question, we performed 12 experiments (a total of about 600 beads) and recorded the number of clusters as a function of their size with time intervals of 5 s. In each experiment, the system was composed of about 50 beads. Initially, the beads were separated a distance $R_i \approx 6$ μm apart. From the images, we could build probability histograms for every 5 s. Figures 7, 8, and 9 show the cluster distributions after 10 s, 20 s, and 30 s, respectively. We note here that the distribution changes from exponential decay to something that appears to be a distorted Gaussian distribution. To understand the time evolution of the probability distribution $P(t)$, we assume that the cluster formation is a Poisson process where

$$P(t) = \frac{(at)^k e^{-at}}{k!} \tag{19}$$

Here k is the cluster size, and we found that $a = (0.18 \pm 0.03)$ s^{-1} is a constant that describes the rate of cluster formation. The circles in Figure 7 show the Poisson distribution after 10

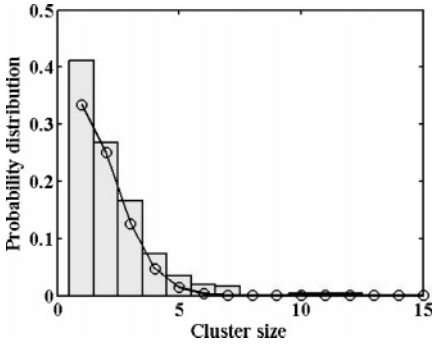

Figure 7. A histogram of the number of beads vs cluster size taken 10 s after turning off the magnetic field. The circles are the corresponding fits using eq 19. Note that the solid line is just a guide for the eyes and the connecting lines do not indicate continuity.

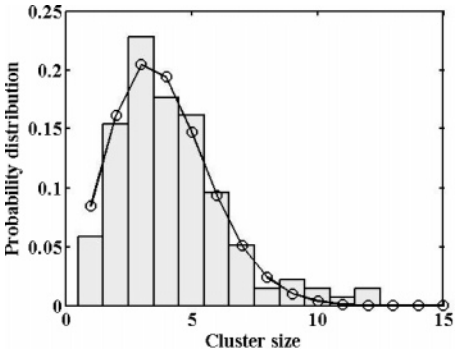

Figure 8. A histogram of the number of beads vs cluster size taken 20 s after turning off the magnetic field. The circles are the corresponding fits using eq 19. Note that the solid line is just a guide for the eyes and the connecting lines do not indicate continuity.

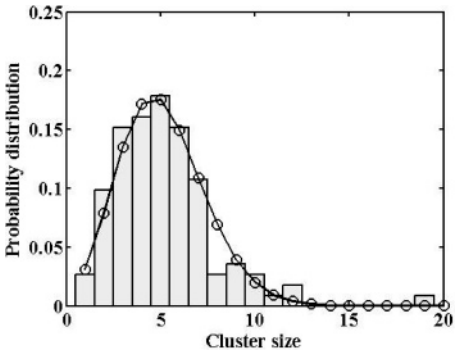

Figure 9. A histogram of the number of beads vs cluster size taken 30 s after turning off the magnetic field. The circles are the corresponding fits using eq 19. Note that the solid line is just a guide for the eyes and the connecting lines do not indicate continuity.

s. We notice that the measured probability drops nearly exponentially with k, in good agreement with eq 19. After 20 s, we see that the distribution has changed and a pronounced peak is seen, again in good quantitative agreement with eq 19. Finally, after 30 s, we notice that the peak has shifted to $k \approx 5$. The distribution now looks more like a Gaussian distribution, as predicted by eq 19. It should be emphasized that the assumption of a Poisson process is only reasonable if the numbers of events in nonoverlapping time intervals are independent random variables. In our case, this may be the case because Brownian motion is assumed to be a main factor responsible for each event. However, we should also point out that capillary forces do play a role and that an accurate understanding of the validity of our assumption requires further analysis.

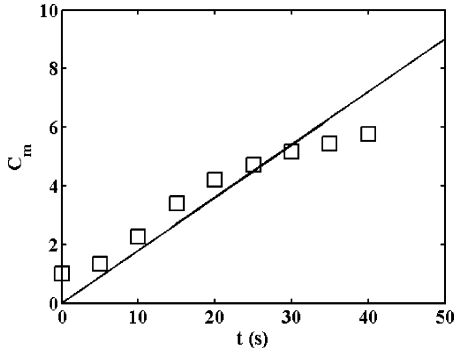

Figure 10. The average cluster size as function of time. The squares show the experimental data, whereas the solid line is a theoretical fit using $C_m = at$, where $a = 0.18\ s^{-1}$.

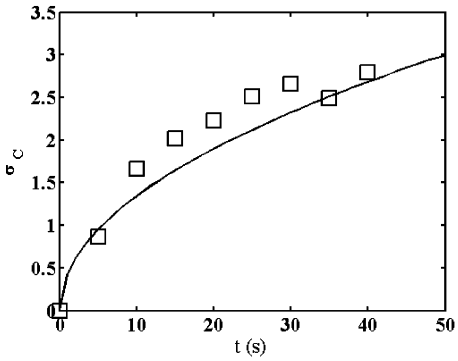

Figure 11. The root-mean-square deviation of the distribution of cluster sizes as a function of time, whereas the solid line corresponds to the theoretical fit using eq 20.

The experiments also allowed us to extract the mean cluster size C_m as function of time, where the average is taken over all the available frames at one instant in time t. The average number of beads in a cluster is also given by the ratio of the total number of colloids (N) to the number of clusters at a particular instant in time (averaged over all the experiments). The experimental data are shown in Figure 10 (squares). According to eq 19, the mean cluster size is given by $C_m = at$, which is shown as a solid line in Figure 10. At $t = 0$ s, our assumptions clearly break down because the experimental distribution is an array of "clusters" containing a single colloid. In the time interval between 5 s and 30 s, it appears that C_m is well explained by a Poisson process, whereas above 30 s, we observe a saturation tendency. It is therefore clear that C_m does not follow the power law one would expect in two- and three-dimensional systems governed by diffusion-limited aggregation.[14−18] We also emphasize that, unlike their two and three-dimensional counterparts, the one-dimensional systems are rather restricted because the beads cannot pass each other, and in our experiments, only a finite reservoir of beads is available.

We also recorded the root-mean-square deviation σ_C of the cluster size as a function of time; see Figure 11 (squares). According to eq 18, the root-mean-square deviation should be given by

$$\sigma_C = \sqrt{at} \tag{20}$$

We note a reasonable good agreement between the experimental data and theoretical fit. However, care should be taken because our system has only a finite number of beads. Thus, one expects σ_C to eventually fall to zero when all the beads again have assembled into a single chain. However, we found

that this took too long, which rendered it difficult to observe such effects with the current system.

6. Conclusion

We have studied diffusion and cluster formation in a finite one-dimensional model system where the particles experience long-range attractive forces. It was shown that the mean-square deviation in distance between the colloids at first increases due to normal Brownian motion, followed by a crossover to anomalous diffusion governed by the long-range forces, thus eventually leading to cluster formation. We also found that the cluster formation can be described as a Poisson process. The results presented here may help us understand diffusion and cluster formation in one-dimensional systems, which may have applications in microfluidics and molecular electronics.

Acknowledgment. I thank L.Y. Chew for helpful comments.

References and Notes

(1) Denkov, N. D.; Velev, O. D.; Kralchevsky, P. A.; Ivanov, I. B.; Yoshimura, H.; Nagayama, K. *Langmuir* **1992**, *8*, 3183.
(2) Helseth, L. E.; Fischer, T. M. *Phys. Rev. E* **2003**, *68*, 051403.
(3) Helseth, L. E.; Fischer, T. M. *Phys. Rev. E* **2003**, *68*, 042601.
(4) Su, G.; Guo, Q.; Palmer, R. E. *Langmuir* **2003**, *19*, 9669.
(5) Cong, H.; Cao, W. *Langmuir* **2003**, *19*, 8177.
(6) Ruiz-García, J.; Gámez-Corrales, R.; Ivlev, B. I. *Phys. Rev. E* **1998**, *58*, 660.
(7) Ruiz-García, J.; Gámez-Corrales, R.; Ivlev, B. I. *Physica A* **1997**, *236*, 97.
(8) Fernandez-Toledano, F.; Moncho-Jordá, A.; Martínez-López, F.; Hidalgo-Álvarez, R. *Langmuir* **2004**, *20*, 6977.
(9) Grzybowski, B. A.; Bowden, N.; Aria, F.; Yang, H.; Whitesides, G. M. *J. Phys. Chem. B* **2001**, *105*, 404.
(10) Grzybowski, B. A.; Whitesides, G. M. *J. Phys. Chem. B* **2001**, *105*, 8770.
(11) Sun, Y.; Walker, Y. C. *J. Phys. Chem. B* **2002**, *106*, 2217.
(12) Guo, Q.; Arnoux, C.; Palmer, R. E. *Langmuir* **2001**, *17*, 7150.
(13) Kralchevsky, P. A.; Denkov, N. D.; Paunov, V. N.; Velev, O. D.; Ivanov, I. B.; Yoshimura, H.; Nagayama, K. *J. Phys.: Condens. Matter* **1994**, *6*, A395.
(14) Hurd, A. J.; Schaefer, D. W. *Phys. Rev. Lett.* **1985**, *54*, 1043.
(15) Helgesen, G.; Skjeltorp, A. T.; Mors, P. M.; Botet, R.; Jullien, R. *Phys. Rev. Lett.* **1988**, *61*, 1736.
(16) Teixeira-Neto, E.; Kaupp, G.; Galembeck, F. *J. Phys. Chem. B* **2003**, *107*, 14255.
(17) Kim, B.; Carignano, M. A.; Tripp, S. L.; Wei, A. *Langmuir* **2004**, *20*, 9360.
(18) Moncho-Jordá, A.; Martínez-López, F.; González, A. E.; Hidalgo-Álvarez, R. *Langmuir* **2002**, *18*, 9183.
(19) González, A. E.; Martínez-López, F.; Moncho-Jordá, A.; Hidalgo-Álvarez, R. *Physica A* **2002**, *314*, 235.
(20) Mougin, K.; Haidara, H. *Langmuir* **2002**, *18*, 9566.
(21) Haidara, H.; Mougin, K.; Schultz, J. *Langmuir* **2001**, *17*, 659.
(22) Yi, D. K.; Seo, E.-M.; Kim, D.-Y. *Langmuir* **2002**, *18*, 5321.
(23) Bhatt, K. H.; Velev, O. D. *Langmuir* **2004**, *20*, 467.
(24) Prieve, D. C. *Adv. Colloid Interface Sci.* **1999**, *82*, 93
(25) Ohshima, Y. N.; Nishio, I. *J. Chem. Phys.* **2001**, *114*, 8649.